Comptes Rendus Geoscience
November-December 2015, Volume 347 (7-8), Pages 377-385
http://dx.doi.org/10.1016/j.crte.2015.04.005
http://archimer.ifremer.fr/doc/00273/38402/

Iron isotope systematics in Arctic rivers

Escoube Raphaelle [1, 2, 9], Rouxel Olivier J. [2, 3, *], Pokrovsky Oleg S. [4, 5, 6], Schroth Andrew [7], Max Holmes Robert [8], Donard Olivier F.X. [1]

[1] LCABIE, Université de Pau et des pays de l'Adour, CNRS UMR 525, Hélioparc, 64053 Pau, France
[2] Department of Marine Chemistry and Geochemistry, Woods Hole Oceanographic Institution, MA 02543 Woods Hole, USA
[3] IFREMER, REM/GM, Centre de Brest, Plouzané, France
[4] Georesources and Environment Toulouse GET, UMR 5563, CNRS, Université Paul-Sabatier, 31400 Toulouse, France
[5] Institute of Ecological Problems of the North, Ural Branch RAS, Arkhangelsk, Russia
[6] BIO-GEO-CLIM Laboratory, Tomsk State University, Tomsk, Russia
[7] Department of Geology, University of Vermont, VT05405 Burlington, USA
[8] Woods Hole Research Center, 02540 Falmouth, MA, USA
[9] Universität zu Köln, Institut für Geologie und Mineralogie, Zülpicher Str. 49b, 50674 Köln, Germany

* Corresponding author : Olivier J. Rouxel, email address : orouxel@ifremer.fr

Abstract :

The input of iron to the Arctic Ocean plays a critical role in the productivity of aquatic ecosystems and is potentially impacted by climate change. We examine Fe isotope systematics of dissolved and colloidal Fe from several Arctic and sub-Arctic rivers in northern Eurasia and Alaska. We demonstrate that the Fe isotopic (δ56Fe) composition of large rivers, such as the Ob' and Lena, has a restricted range of δ56Fe values ca.–0.11 ± 0.13‰, with minimal seasonal variability, in stark contrast to smaller organic-rich rivers with an overall δ56Fe range from–1.7 to + 1.6‰. The preferential enrichment with heavy Fe isotopes observed in low molecular weight colloidal fraction and during the high-flow period is consistent with the role of organic complexation of Fe. The light Fe isotope signatures of smaller rivers and meltwater reflect active redox cycling. Data synthesis reveals that small organic-rich rivers and meltwater in Arctic environments may contribute disproportionately to the input of labile Fe in the Arctic Ocean, while bearing contrasting Fe isotope compositions compared to larger rivers.

Keywords : Iron isotope, Colloids, River, Weathering, Arctic, Iron speciation

1. Introduction

The boreal zone of the Russian Arctic and glacierized systems of Greenland and Alaska are systems that are currently experiencing rapid environmental change associated with climate change. The observed warming in the arctic is much greater than the global average (IPCC, 2007) and on-going permafrost thaw is considered to induce large perturbations on the global water discharge and organic carbon inventory in arctic rivers (Dittmar and Kattner, 2003, Holmes et al., 2012) as well as the flux and speciation of trace elements input into the Arctic Ocean (Pokrovsky and Schott, 2002, Pokrovsky et al., 2012, Pokrovsky et al., 2010). The Arctic Ocean receives about 10% of the global river discharge, yet it has the highest input of continental freshwater per basin surface area compared to all other world's oceans. In addition, the three largest arctic rivers, the Yenisey, Lena, and Ob' are each comparable in watershed area and annual discharge to the Mississippi River (Holmes et al., 2012).

Riverine iron (Fe) plays a critical role in regulating the concentration and bioavailability for a variety of chemical elements in aquatic ecosystems, including nutrients and pollutants. In general, the behavior of Fe and its partitioning between dissolved, colloidal, and suspended sediment loads is controlled by local hydrogeochemical and biogeochemical environments which are themselves likely to be affected by climate change (Allard et al., 2004, Schroth et al., 2009). Likewise, glacial weathering has been recently recognized as a primary source of Fe and other nutrients (phosphate, dissolved organic matter) to the highly productive coastal ecosystems of the Gulf of Alaska (Crusius et al., 2011, Schroth et al., 2011) and enhanced iron input has been observed during high run-off periods of snowmelt in spring and glacial melt in the summer. Understanding the mechanisms and external forcing of Fe delivery into the Arctic Ocean therefore requires: (1) time-series-based analyses of arctic and subarctic river biogeochemistry to assess climatic and seasonnally-driven variations, (2) assessment of the speciation and mobility of Fe in high-latitude watershed, (3) determination of the potential impact of glacier or permafrost thaw on the speciation, timing and provenance of Fe input to the high- lattitude oceans.

A growing number of studies have reported Fe isotope composition of bulk rivers, as well as particulate, dissolved and colloids Fe pools in rivers (Bergquist and Boyle, 2006, Escoube et al., 2009, Fantle and DePaolo, 2004, Ilina et al., 2013, Ingri et al., 2006, Pinheiro et al., 2014, Pinheiro et al., 2013, Poitrasson et al., 2014, Schroth et al., 2011, Chen et al, 2014). Results showed significant variability in Fe isotopes which have been attributed to a range of processes and parameters, including hydrology, climate and anthropogenic influences, as well as bedrock geology, topography, and soil-plant interactions. To date, only two studies have reported the isotope composition of dissolved Fe in arctic/subarctic environments (i.e. referred as $\delta^{56}Fe_{DFe}$, with DFe for dissolved Fe < 0.45 or < 0.22 µm) that yielded one of the largest range observed in river systems, between -1.2 and 1.8 ‰ (Ilina et al., 2013, Schroth et al., 2011). Lightest $\delta^{56}Fe_{DFe}$ values were reported for organic-rich rivers and streams draining area with the largest vegetal cover in Alaska (Schroth et al., 2011) while heaviest values were measured in colloidal and dissolved fractions of boreal and temperate organic-rich rivers in Karelia (Ilina et al., 2013).

Here, we investigate Fe isotope systematics in northern European and Siberian rivers (**Figure 1**), including (1) a time-series of $\delta^{56}Fe_{DFe}$ of two of the largest rivers draining arctic watersheds (the Ob' and Lena) focusing on the peak flow that provides a first order assessment of the annual Fe budgets; and (2) $\delta^{56}Fe$ values of colloidal and suspended pools (ranging from 1 kDa to 1.2 µm) of smaller northern European rivers, including the Severnaya Dvina River to assess the influence of Fe-rich colloids on the Fe isotopic composition of freshwater sources in the Arctic. We further compare the results with our previously reported Fe isotope composition of Alaskan rivers (Schroth et al., 2011) to determine how Fe isotope signatures may vary among high-latitude watersheds. Without such characterization of the present state of the system, future changes in the response of these river systems to global change cannot be properly evaluated.

2. Materials

Field sampling of the Ob' and Lena have been performed by the Arctic Great Rivers Observatory during the 2007 baseflow to high flow transition as reported by Holmes et al. (2012). Sampling sites were located the nearest to the river mouths at Salekhard for Ob’ and Zhigansk for Lena. With a discharge of 427 km^3/yr and 588 km^3/yr respectively, the Ob’ and Lena represent 18 and 25 % of riverine freshwater inputs to the Arctic Ocean (Holmes et al., 2012).

Rivers draining into the White Sea (between latitudes 67°N and 63°N and longitudes 30°E and 36°E) were sampled in the boreal and subarctic region of the European Russia. This region typically experiences a very large range of temperature varying from -50°C to 30°C between winter and summer. The mean annual river discharge in the White Sea is 231 km^3/yr; from whose 47% correspond to the Severnaya Dvina watershed (Pokrovsky et al., 2010). Sampled sites are on unpopulated area and represent a diverse collection of geochemical environments with bedrock lithologies ranging from granites, basalts, ultramafic rocks, and carbonate-rich sediments (*Table S1, Supplementary Material*) and hydrological settings (soil depression, river, bog and meltwater). Based on geographic location, we divided the studied area into three zones: (i) Yukova watershed, including the Yukova, Ladreka and Ruiga Rivers and stagnant waters; (ii) Peschanaya River and pit water; and (iii) the Severnaya Dvina, including its tributaries Pinega River and Sotkas River as well as local bog water.

Samples from the Yukova (zone 1) were collected from small streams or rivers and stagnant water (e.g. ice, pit water). The Peschanaya (zone 2) is a pristine river draining to the Kuloy estuary of the White Sea. Water samples were collected during August 2006 and are affected by the input of peat bogs and swamps. The Severnaya Dvina (zone 3) was sampled in 2007 during 3 contrasted hydrological regimes: at the end of February, representing the baseflow winter conditions; in the beginning of May when most of the thawing occurred; and the middle of June, at the beginning of summer baseflow conditions (Pokrovsky et al., 2010). In general, the spring flood (snow melt) lasts from 30 to 50 days and contributes to about 60% of the annual water flux.

Additional river, stream and meltwater samples from Alaska were analysed as part of the sample set previously reported by Schroth et al. (2011) (*Table S2, Supplementary Material)*. Four broad classes of tributaries representative of main landscape of the Copper River watershed were sampled in August and October 2008, and include: (1) Glacial tributaries that are milky brown in appearance, indicative of extremely high suspended sediment loads corresponding to the contribution of glacial meltwater; (2) Proglacial tributaries fed by lake developed at the terminus of the glacier; (3) Boreal forested montane streams that are not glacierized and have relatively low suspended sediment loads; (4) Boreal forested ‘blackwater’ tributaries draining large lowland areas in the Copper River basin and delta, with high concentrations of organic compounds. All samples from glacierized catchments were collected under peak glacial melt in August of 2008, while forested catchments were sampled concurrently, but under summer baseflow conditions due to the lack of input from glacial ice in those systems.

3. Methods

The full description of the sampling and filtration methods and the geochemical data for the Ob', Lena, White Sea area and Alaska rivers are presented in the supplementary online materials. Fe isotopes and elemental analyses were performed on a range of suspended, dissolved and colloidal fractions filtered through 2.5 μm to < 1kDa.

4. Results

4.1. Comparison of ultrafiltration systems

It is well-recognized that ultrafiltration techniques may induce analytical artifacts due to charge separation, diffusion and clogging of the filter membrane (Dupré et al., 1999, Viers et al., 1997). Potential Fe isotope fractionation artefacts have been already discussed in previous studies (Ilina et al., 2013). As shown in **Figure 2**, colloid sizes < 10 kD and < 1 kD separated using pressure ultrafiltration (UF) show an enrichment in heavy Fe isotopes by 0.26 to 0.37‰ compared with colloid sized separated through dialysis membrane (Dial) (Spectra Por 7) via passive diffusion. Hence, it is possible that separation by dialysis enriches the filtrate solution in light Fe isotopes, which is expected during diffusion mechanisms. However, this difference is of second order importance when compared to the overall range of δ^{56}Fe observed between dissolved Fe (< 0.2 μm) and colloidal Fe in most samples (e.g. #23, Y-3, Y-1, Y-5). In addition, because of the differences of techniques and potential filter clogging effects, dialysis and pressure ultrafiltration may not separate the same types of colloids.

4.2. Fe isotope composition of waters from White Sea area

In the Yukovo system, winter $\delta^{56}Fe_{DFe}$ values show systematically positive values from 0.24‰ for sample Y-3 to 0.79‰ for sample Y-1 (**Figure 2**). Colloidal (<100 kDa and <10 kDa) and truly dissolved or soluble (i.e. low molecular weight) fractions (<1 kDa) of samples Y-1 and Y-3 also show systematic enrichment in heavy Fe isotopes relative to DFe (increase by up to 0.79‰ for Y-1 and 0.62‰ for Y-3). The enrichment in heavy isotopes is also associated with a drastic decrease of Fe concentration between DFe and soluble fraction (from 535 to 25 µg/L for Y-1 and 1117 to 46 µg/L for Y-3). Stagnant water (sample Y-4) and meltwater (sample Y-5) show lighter $\delta^{56}Fe$ values for colloidal fractions, with $\delta^{56}Fe_{FeD}$ values as low as -1.29‰ and -0.83‰ respectively (**Figure 2**). It is important to note that Y-4, which corresponds to stagnant water trapped between two ice layers, also yields the highest Fe and Mn concentration and the most negative $\delta^{56}Fe$ values for both suspended and dissolved pools (*Table S4*). Other samples from the same area (Ruiga #23 and Ladreka #9) recovered in the summer show a similar trend toward heavier $\delta^{56}Fe$ values for smaller colloidal pools, although lighter $\delta^{56}Fe$ values (down to -0.07‰) are observed for <1kDa fraction in the Ruiga (**Figure 2**). The Peschanaya waters (zone 2) yield $\delta^{56}Fe_{DFe}$ values between -0.3 and -0.24‰ (samples s-32 and s-40 respectively), with slightly heavier value measured for truly dissolved Fe ($\delta^{56}Fe$ = -0.07‰, *Table S4*).

The Severnaya Dvina (zone 3) was sampled over contrasting hydrological conditions. In general, this river is characterized by lower DOC contents showing a significant increase during the spring period, consistent with the release of organic-rich materials during high flow. In contrast, Fe concentrations appear unrelated to changes of hydraulic regimes. $\delta^{56}Fe_{DFe}$ yield near-zero values during baseflow (i.e. -0.01‰ for samples A-3 and A-28) while heavier $\delta^{56}Fe_{DFe}$ value up to 0.55‰ (sample A-18) is obtained during high flow. Similar increases in $\delta^{56}Fe_{DFe}$ values during high flow period are also observed for the Pinega River, while identical values were obtained between high and base flow in the Sotka River. Colloidal fractions in rivers (A-3, A-18, A7) generally show a trend toward heavy Fe isotope enrichment in smaller size colloids (**Figure 2**).

4.3. Alaska Rivers

Preliminary $\delta^{56}Fe_{DFe}$ values of rivers from the Copper River watershed have been previously presented in Schroth et al. (2011). Additional values reported here include $\delta^{56}Fe_{DFe}$ measured on a larger set of rivers and for different filtration pore size (i.e. 0.45 and 0.02 µm filters) (**Figure 3**). In glacial and proglacial lake-fed tributary systems, the Fe isotopic signatures are similar to crustal values defined as 0.09‰ (±0.1‰) (Beard et al., 2003, Dauphas and Rouxel, 2006). In contrast, the boreal-forested systems display much lighter $\delta^{56}Fe$ values down to -1.73‰, which also correspond to higher concentrations of DOC (Schroth et al., 2011).

4.4. Fe isotope composition of large arctic rivers

Time series samples of the Ob' and Lena rivers were collected to capture the transition between baseflow and high flow (**Figure 4**). In arctic environment, the water discharge peak lasted a few hours to days, leading to an extremely small sampling window. For the Lena River, sampling started just before the peak of discharge while for the Ob' River, discharge rates remained essentially constant, suggesting that the system return rapidly to low flow conditions. Average $\delta^{56}Fe_{DFe}$ values of both rivers are essentially identical within uncertainty, yielding $\delta^{56}Fe_{DFe}$ = -0.11 ± 0.13‰ (2sd, n=15 for the Lena, and n=20 for the Ob'). The total range of $\delta^{56}Fe_{DFe}$ is restricted to 0.23‰ for Lena River and 0.30‰ for Ob' River, showing a lack of relationships between Fe isotope composition and discharge evolution. For the Ob' River, lighter $\delta^{56}Fe_{DFe}$ values (from -0.29 to -0.10‰) are measured at the beginning of the sampling period when discharge rate is slightly higher (from 3.2 to 3.0 km^3/d), but this trend is not observed for the Lena River where changes of discharge rates are larger (from 2.1 to 9.5 km^3/d).

5. Discussion

Variable $\delta^{56}Fe_{DFe}$ values have been already reported in rivers from temperate and tropical environments, with a total range from -0.7 to 0.8‰ (see Figure S1, supplementary material). Although early studies proposed that dissolved Fe in rivers had $\delta^{56}Fe_{DFe}$ values lighter than bulk continental crust (Bergquist and Boyle, 2006, Fantle and DePaolo, 2004), more recent studies have identified ubiquitous heavy $\delta^{56}Fe_{DFe}$ in organic-rich rivers of temperate region and in the Arctic (Escoube et al., 2009, Ilina et al., 2013). Analysis of our new dataset supports the recent study of Ilina et al. (2013), confirming that DFe and colloidal Fe in arctic rivers display an extreme range of $\delta^{56}Fe_{DFe}$ from -1.4‰ to 2‰. This suggests that a dynamic and complex partitioning of Fe isotopes between particulate, colloidal and 'dissolved' fractions, which may be unique to high latitude river networks.

In the Copper River watershed in Alaska, systematically lighter $\delta^{56}Fe_{DFe}$ values are commonly observed in organic carbon- and Fe-rich boreal rivers, while glacial rivers do not show significant fractionation relative to bulk crust (**Figure 3** and **5**). An important exception includes a small river draining montane boreal forest (i.e. Tractor creek) showing heavier values up to 0.68‰ (**Figure 3**). Glacial rivers characterized by near crustal $\delta^{56}Fe$ should mainly reflect the contribution of particles and colloids derived from physical erosion, where the mechanical transport of lithogenic materials should proceed with minimal Fe isotope fractionation. In this case, the slight enrichment in heavy isotopes observed in some glacial rivers could be attributed to the alteration of specific lithologies, such as shales recognized as potential source of heavy Fe (Yesavage et al., 2012) or isotopically heavy crystalline rocks such as granite (Poitrasson and Freydier, 2005).

The lighter $\delta^{56}Fe_{DFe}$ values of boreal forested rivers has been previously interpreted to reflect either the contribution of groundwater and/or soil water-derived Fe with DOC derived from organic matter decomposition (Schroth et al., 2011). It has been experimentally demonstrated that equilibrium Fe-organic complexation would favor heavy Fe isotopes in organically-bound Fe (Dideriksen et al., 2008) while kinetic mineral dissolution in the presence of Fe chelating organic ligands would favor the release of light Fe into solution (Brantley et al., 2001, Kiczka et al., 2010a). Plant uptake may also favour light Fe isotopes that may be released to rivers after the decomposition of soil organic matter (Kiczka et al., 2010b). Additional constraints on the origin of isotopically light Fe in organic-rich rivers may be derived from our new data from ice meltwater and time-series, as discussed below.

Several lines of evidence suggest that dissolved Fe in ice meltwater is enriched in light isotope. In the Alaska system, glacial meltwater (sample #St32) shows $\delta^{56}Fe_{DFe}$ = -0.81‰, while labile (< 10 kDa) and fine particulate Fe (< 2.5 µm) from water trapped in ice from the White Sea area (sample Y-4) show $\delta^{56}Fe$ ranging from -1.04 to -1.28‰. Light $\delta^{56}Fe_{DFe}$ values have been also reported in Antarctic sea ice particulate matter and dissolved Fe, with values probably lower than -1.5‰ (de Jong et al., 2007). These light values have been interpreted as reflecting the presence of heterotrophs in the upper layers with predominantly flagellates and bacteria. Here, we propose instead that the generally light $\delta^{56}Fe$ in meltwater is mainly the result of redox effects rather than biological uptake. The overall enrichments in Fe and Mn in sample Y-4, associated with the lightest $\delta^{56}Fe$ values (**Table S4**), suggest the contribution of anoxic to suboxic water. Sample Y-4 is trapped between two ice layers and is therefore isolated from the atmosphere allowing reducing conditions to build up, promoting the release of labile Mn(II) and Fe(II) during the degradation of particulate organic matter by heterotrophic organisms. Considering the *ca.* 3‰ fractionation factors between Fe^{II} and Fe^{III} (Welch et al., 2003, Wu et al., 2011), Fe(II) is expected to be enriched in light isotopes relative to Fe(III) remaining in the suspended particles. Similar processes involving Fe redox cycling have been well identified during diagenetic reactions in marine sediments and porewater (Homoky et al., 2009, Rouxel et al., 2008, Severmann et al., 2006) as well as during redox-controlled release of Fe in soils (Schuth et al., 2015), which also likely occurs during the formation of meltwater (Bhatia et al., 2013).

It has been recently shown that glacial runoff may provide a significant source of bioavailable iron to surrounding coastal oceans as a result of ice melting (Bhatia et al., 2013). Two mechanisms have been proposed to explain the increase of dissolved Fe concentration in runoff meltwater, including the contribution of Fe-rich hypoxic or anoxic water in the subglacial drainage system or an increase of DOC concentrations. Based on our results, it seems that Fe isotope systematics may provide means to distinguish between these two mechanisms. When Fe is bound to organic ligands (i.e. DOC), it should be enriched in heavy isotopes (e.g. Dideriksen et al., 2008). In contrast, when Fe is released from oxygen-depleted meltwater, it should be enriched in light isotopes.

The small organic-rich rivers from the White Sea watershed (Severnaya and Pinega Rivers) show heavier Fe isotope values during high discharge periods and for small-size colloids (**Figure 2**, *Table S4*). Differences in $\delta^{56}Fe_{DFe}$ of up to 0.6‰ and 0.7‰ have been reported for Severnaya and Pinega Rivers between low- and high- flow. Soluble fractions (<1kDa) also show systematic enrichment in heavy Fe isotopes relative to DFe (e.g. increase by up to 0.79‰ for sample Y-1). As discussed previously (Ilina et al., 2013), heavier δ^{56}Fe values in small arctic rivers should mainly reflect a larger contribution of organic-rich small colloids that undergo seasonal recycling and mixing between different colloidal sources. Heavier δ^{56}Fe values are therefore consistent with the complexation of Fe(III) with strong organic chelates as confirmed experimentally by Dideriksen et al. (2008), although sedimentary rock weathering (e.g. shale) may also provide an alternate source of isotopically heavy colloidal Fe in rivers due to incongruent dissolution mechanisms (Yesavage et al., 2012). The later hypothesis may also explain the significant fractionation of Fe vs Al between different colloid sizes. The overall decrease of Fe/Al ratios for smaller colloid size with a concomitant increase in δ^{56}Fe (**Figure 2**) suggests the existence of Fe-depleted and isotopically heavy reservoir generated by multiple alteration stages. This hypothesis is also consistent with the lack of inverse correlation between δ^{56}Fe and DOC (or DOC/Fe) (**Figure 5**), suggesting rather a large range of δ^{56}Fe values in organic-rich colloids from the White Sea watershed).

By comparison, the relatively constant δ^{56}Fe values of the Lena and Ob' Rivers over time (δ^{56}Fe = -0.11 ± 0.13‰) contrast with the large variability observed in smaller river systems, either from temperate, tropical or boreal regions. Considering that Ob' and Lena samples show similar or even higher enrichment in DOC (10 to 20 mg C/L) than organic-rich rivers from boreal-forested rivers (Schroth et al., 2011) (**Figure 5**) and even tropical rivers (Bergquist and Boyle, 2006), the small Fe isotope fractionation of *ca.* -0.2‰ relative to bulk crust is surprising. Presumably, the release of Fe-rich colloids during the peak discharge does not allow significant particulate-dissolved isotope exchange as observed in smaller organic-rich riverine systems. This suggests the absence of a significant contribution of fractionated reservoir in larger arctic rivers derived from anoxic swamps and meltwater or from plant litter decay in summer. Alternatively, this could be also interpreted as an integrated signal from these fractionated reservoirs whose relative contributions stay similar throughout the hydrologic year. This contrasts with smaller rivers where shorter flowpaths would produce variable mixing ratios of these sources and therefore more variable Fe isotopic compositions. Alaskan rivers also support this hypothesis since the Copper River shows homogeneous δ^{56}Fe values despite the variable δ^{56}Fe values measured in its tributaries..

The variations of dissolved and particulate δ^{56}Fe values have been generally attributed to distinct weathering processes and environmental parameters (Pinheiro et al., 2014, Pinheiro et al., 2013, Poitrasson et al., 2014, Song et al., 2011). It has been also proposed that Fe isotope composition of suspended particulate matter is possibly linked to climatic conditions, with high latitude rivers exhibiting mostly positive δ^{56}Fe values, while tropical rivers showing strongly negative Fe isotopic signatures (Pinheiro et al., 2014). Our new data suggest that this model does not necessarily apply to large rivers such as the Ob' and Lena. Isotopically light organic-rich rivers may also occur in subarctic climate as those reported in the Copper River watershed in Alaska.

6. Concluding perspectives on the global flux of Fe isotopes in arctic environments

The impact of global warming on permafrost degradation in the Arctic has received considerable attention (Dittmar and Kattner, 2003, Frey and McClelland, 2009, O'Donnell et al., 2012, Romanovsky et al., 2010). Permafrost-driven changes in watershed hydrology have been accounted for the increased flux of dissolved organic carbon from terrestrial to aquatic and marine ecosystems, in relation to basin-wide permafrost thaw and an increase in groundwater contribution in base flow. An important feature of all boreal catchments is the large flux of dissolved and particulate matter and especially organic carbon occurring during relatively short high-flow period of snowmelt (Holmes et al., 2012, Pokrovsky et al., 2010).

Considering the combined annual water discharge of the Ob' and Lena of 1015 km^3/yr (Holmes et al., 2012), corresponding to *ca.* 40% of the global riverine flux in the Arctic Ocean, our study allows the first estimation of the Fe isotope composition of riverine dissolved Fe flux in the Arctic Ocean. To our knowledge, the annual fluxes of Fe from the Ob' and Lena have not been reported in previous studies. Hence, at a first approximation, we consider that Fe flux is proportional to DOC flux, with relationships of Fe/DOC = 21 ± 6 (g/kg) for Lena river and 61 ± 8 (g/kg) for Ob' river (*Table S3*). Although Fe enrichment in rivers is often associated with organic or humic-rich colloids (Allard et al., 2004), the long-term relationship between DOC and Fe in these rivers should be however used with caution. Using the annual DOC fluxes determined in previous studies (Holmes et al., 2012), we determine a total annual flux of dissolved Fe of 84 ± 25 (10^9 g/yr) for Lena river and 252 ± 34 (10^9 g/yr). By normalizing $\delta^{56}Fe_{DFe}$ to Fe fluxes, we further determine the annual discharge of Fe having $\delta^{56}Fe_{DFe}$ = -0.110‰ for Lena river and $\delta^{56}Fe_{DFe}$ = -0.112‰ for Ob' river. These values suggest that large rivers, contributing to the largest input of freshwater into the Arctic Ocean, have very homogeneous $\delta^{56}Fe_{DFe}$ values, slightly enriched in light isotopes by 0.2‰ relative to bulk continental crust. The similarities of average $\delta^{56}Fe_{DFe}$ between these two large rivers is interesting considering their contrasted permafrost coverage, totalling 4% for Ob' river and 90% for Lena river (Holmes et al., 2012). Although spring flow period is not the most affected by permafrost thaw, our results argue against significant influence of permafrost degradation on Fe isotope composition of DFe in subarctic rivers.

In contrast, smaller arctic river systems show much larger spread in $\delta^{56}Fe_{DFe}$ values, with a marked enrichment in heavy Fe isotopes up to 0.55‰ during spring flood period and for small colloids. The Severnaya Dvina is the largest European subarctic river, contributing to 4% of the total water discharge to the Arctic Ocean (e.g. Pokrovsky et al., 2010). The estimated total annual DFe flux from the Severnaya Dvina has been previously determined to 53 ± 16 10^9 g/yr (Pokrovsky et al., 2010), which is more than 50% the total Fe flux of the Lena. Hence, smaller arctic rivers may contribute disproportionately to the input of DFe in the Arctic Ocean, while showing strongly fractionated (i.e. heavier) Fe isotope values. Since the Severnaya Dvina drains both silicate-bearing and carbonate rocks, similar source of heavy DFe may be commonly observed in other remote rivers of the Arctic. It has been also recently demonstrated that the most labile Fe fraction (i.e. <1kDa) in arctic rivers increases its concentration by a factor of 5 during estuarine mixing (Pokrovsky et al., 2014). Hence, the labile and potentially bioavailable Fe in small organic-rich arctic and subarctic rivers may provide an important source of both isotopically light and heavy Fe to the Arctic Ocean, with δ^{56}Fe values as high as 2.7 ‰ (Ilina et al., 2013) and as low as -1.7‰.

We interpret the striking contrast of Fe isotope signatures between large vs. smaller organic-rich arctic rivers to be influenced by the fact that smaller rivers tend to have more northerly watersheds, therefore integrating a smaller number of Fe sources. Hence, element source and biogeochemical cycling may be considerably different than for the larger rivers, such as Ob' and Lena whose watersheds extending much further south. Seasonal measurements of Fe and other element concentrations and speciation reveal the presence of two main sources of Fe that are preferentially mobilized and disproportionaltely influence riverine Fe loads under different conditions during the high-latitude hydrologic year (Pokrovsky et al., 2010): 1) deep groundwaters poor in organic matter and 2) colloids and organic-rich surficial soil waters. These sources should have contrasted $\delta^{56}Fe_{DFe}$ values, with isotopically light $\delta^{56}Fe_{DFe}$ values for groundwater-derived Fe on the one hand, and isotopically heavy $\delta^{56}Fe_{DFe}$ values for soil-derived organic-rich colloids on the other hand. The impact of climate change in the Arctic may therefore differ among these classes of rivers and Fe sources, producing contrasted and evolving Fe isotope composition for global Fe delivery in the Arctic Ocean.

Acknowledgment

This work was supported by the National Science Foundation (OCE 0550066), WHOI Arctic Research Initiative, Labex Mer (ANR-10-LABX-19-01), and FP7 (#247837), RFFI No 13-05-00890, 14-05-98815 and BIO-GEO-CLIM No 14.B25.31.0001 grants. This work would not have been possible without the initial collaborations with Bernhard Peucker-Ehrenbrink and John Crucius. Christian Miller. We also thank Lary Ball, Jurek Blustajn, Fanny Chever, Emmanuel Ponzevera and Maureen Auro for their technical support. We thank Sébastien Bertrand, Bernhard Peucker-Ehrenbrink, Valier Galy, Catherine Jeandel and Francois Lacan for helpful discussions and Marc Benedetti and Vincent Busigny for helpful comments on the manuscript.

Bibliography

Allard, T., Menguy, N., Salomon, J., Calligaro, T., Weber, T., Calas, G., Benedetti, M.F., 2004. Revealing forms of iron in river-borne material from major tropical rivers of the Amazon Basin (Brazil). Geochimica et Cosmochimica Acta, 68: 3079-3094.

Beard, B.L., Johnson, C.M., Skulan, J.L., Nealson, K.H., Cox, L., Sun, H., 2003. Application of Fe isotopes to tracing the geochemical and biological cycling of Fe. Chemical Geology, 195: 87-117.

Bergquist, B.A., Boyle, E.A., 2006. Iron isotopes in the Amazon River system: Weathering and transport signatures. Earth and Planetary Science Letters, 248: 54-68.

Bhatia, M.P., Kujawinski, E.B., Das, S.B., Breier, C.F., Henderson, P.B., Charette, M.A., 2013. Greenland meltwater as a significant and potentially bioavailable source of iron to the ocean. Nature Geoscience, 6: 274-278.

Brantley, S.L., Liermann, L., Bullen, T.D., 2001. Fractionation of Fe isotopes by soil microbes and organic acids. Geology, 29: 535-538.

Crusius, J., Schroth, A.W., Gasso, S., Moy, C.M., Levy, R.C., Gatica, M., 2011. Glacial flour dust storms in the Gulf of Alaska: Hydrologic and meteorological controls and their importance as a source of bioavailable iron. Geophysical Research Letters, 38:

Dauphas, N., Rouxel, O., 2006. Mass spectrometry and natural variations of iron isotopes. Mass Spectrometry Reviews, 25: 515-550.

de Jong, J., Schoemann, V., Tison, J.L., Becquevort, S., Masson, F., Lannuzel, D., Petit, J., Chou, L., Weis, D., Mattielli, N., 2007. Precise measurement of Fe isotopes in marine samples by multi-collector inductively coupled plasma mass spectrometry (MC-ICP-MS). Analytica Chimica Acta, 589: 105-119.

Dideriksen, K., Baker, J.A., Stipp, S.L.S., 2008. Equilibrium Fe isotope fractionation between inorganic aqueous Fe(III) and the siderophore complex, Fe(III)-desferrioxamine B. Earth and Planetary Science Letters, 269: 280-290.

Dittmar, T., Kattner, G., 2003. The biogeochemistry of the river and shelf ecosystem of the Arctic Ocean: a review. Marine Chemistry, 83: 103-120.

Dupré, B., Viers, J., Dandurand, J.-L., Polve, M., Benezeth, P., Vervier, P., Braun, J.-J., 1999. Major and trace elements associated with colloids in organic-rich river waters: ultrafiltration of natural and spiked solutions. Chem. Geol., 160: 63-80.

Escoube, R., Rouxel, O.J., Sholkovitz, E., Donard, O.F.X., 2009. Iron isotope systematics in estuaries: The case of North River, Massachusetts (USA). Geochimica Et Cosmochimica Acta, 73: 4045-4059.

Fantle, M.S., DePaolo, D.J., 2004. Iron isotopic fractionation during continental weathering. Earth and Planetary Science Letters, 228: 547-562.

Frey, K.E., McClelland, J.W., 2009. Impacts of permafrost degradation on arctic river biogeochemistry. Hydrological Processes, 23: 169-182.

Holmes, R.M., McClelland, J.W., Peterson, B.J., Tank, S.E., Bulygina, E., Eglinton, T.I., Gordeev, V.V., Gurtovaya, T.Y., Raymond, P.A., Repeta, D.J., Staples, R., Striegl, R.G., Zhulidov, A.V., Zimov, S.A., 2012. Seasonal and Annual Fluxes of Nutrients and Organic Matter from Large Rivers to the Arctic Ocean and Surrounding Seas. Estuaries and Coasts, 35: 369-382.

Homoky, W.B., Severmann, S., Mills, R.A., Statham, P.J., Fones, G.R., 2009. Pore-fluid Fe isotopes reflect the extent of benthic Fe redox recycling: Evidence from continental shelf and deep-sea sediments. Geology, 37: 751-754.

Hood, E., Scott, D., 2008. Riverine organic matter and nutrients in southeast Alaska affected by glacial coverage. Nature Geoscience, 1: 583 - 587.

Ilina, S.M., Poitrasson, F., Lapitskiy, S.A., Alekhin, Y.V., Viers, J., Pokrovsky, O.S., 2013. Extreme iron isotope fractionation between colloids and particles of boreal and temperate organic-rich waters. Geochimica Et Cosmochimica Acta, 101: 96-111.

Ingri, J., Malinovsky, D., Rodushkin, I., Baxter, D.C., Widerlund, A., Andersson, P., Gustafsson, Ö., Forsling, W., Öhlander, B., 2006. Iron isotope fractionation in river colloidal matter. Earth and Planetary Science Letters, 245: 792-798.

IPCC, Climate change 2007: The physical science basis. Contribution of working group I to the fourth assessment report of the intergovernmental panel on climate change, in: S. Solomon, D. Qin, M. Manning, Z. Chen, M. Marquis, K.B. Averyt, M. Tignor (Eds.), 2007.

Kiczka, M., Wiederhold, J.G., Frommer, J., Kraemer, S.M., Bourdon, B., Kretzschmar, R., 2010a. Iron isotope fractionation during proton- and ligand-promoted dissolution of primary phyllosilicates. Geochimica Et Cosmochimica Acta, 74: 3112-3128.

Kiczka, M., Wiederhold, J.G., Kraemer, S.M., Bourdon, B., Kretzschmar, R., 2010b. Iron Isotope Fractionation during Fe Uptake and Translocation in Alpine Plants. Environmental Science & Technology, 44: 6144-6150.

O'Donnell, J.A., Aiken, G.R., Walvoord, M.A., Butler, K.D., 2012. Dissolved organic matter composition of winter flow in the Yukon River basin: Implications of permafrost thaw and increased groundwater discharge. Global Biogeochemical Cycles, 26:

Pinheiro, G.M.D., Poitrasson, F., Sondag, F., Cochonneau, G., Vieira, L.C., 2014. Contrasting iron isotopic compositions in river suspended particulate matter: the Negro and the Amazon annual river cycles. Earth and Planetary Science Letters, 394: 168-178.

Pinheiro, G.M.D., Poitrasson, F., Sondag, F., Vieira, L.C., Pimentel, M.M., 2013. Iron isotope composition of the suspended matter along depth and lateral profiles in the Amazon River and its tributaries. Journal of South American Earth Sciences, 44: 35-44.

Poitrasson, F., Freydier, R., 2005. Heavy iron isotope composition of granites determined by high resolution MC-ICP-MS. Chemical Geology, 222: 132-147.

Poitrasson, F., Vieira, L.C., Seyler, P., Pinheiro, G.M.D., Mulholland, D.S., Bonnet, M.P., Martinez, J.M., Lima, B.A., Boaventura, G.R., Chmeleff, J., Dantas, E.L., Guyot, J.L., Mancini, L., Pimentel, M.M., Santos, R.V., Sondag, F., Vauchel, P., 2014. Iron isotope composition of the bulk waters and sediments from the Amazon River Basin. Chemical Geology, 377: 1-11.

Pokrovsky, O.S., Schott, J., 2002. Iron colloids/organic matter associated transport of major and trace elements in small boreal rivers and their estuaries (NW Russia). Chem. Geol., 190: 141-179.

Pokrovsky, O.S., Shirokova, L.S., Viers, J., Gordeev, V.V., Shevchenko, V.P., Chupakov, A.V., Vorobieva, T.Y., Candaudap, F., Causserand, C., Lanzanova, A., Zouiten, C., 2014. Fate of colloids during estuarine mixing in the Arctic. Ocean Science, 10: 107-125.

Pokrovsky, O.S., Viers, J., Dupré, B., Chabaux, F., Gaillardet, J., Audry, S., Prokushkin, A.S., Shirokova, L.S., Kirpotin, S.N., Lapitsky, S.A., Shevchenko, V.P., 2012. Biogeochemistry of major and trace elements in watersheds of Northern Eurasia drained to the Arctic Ocean: The change of fluxes, sources and mechanisms under the climate warming prospective. C.R. Acad. Sci. Paris, doi: 10.1016/j.crte.2012.1008.1003.

Pokrovsky, O.S., Viers, J., Shirokova, L.S., Shevchenko, V.P., Filipov, A.S., Dupre, B., 2010. Dissolved, suspended, and colloidal fluxes of organic carbon, major and trace elements in the Severnaya Dvina River and its tributary. Chemical Geology, 273: 136-149.

Romanovsky, V.E., Smith, S.L., Christiansen, H.H., 2010. Permafrost Thermal State in the Polar Northern Hemisphere during the International Polar Year 2007-2009: a Synthesis. Permafrost and Periglacial Processes, 21: 106-116.

Rouxel, O., Sholkovitz, E., Charette, M., Edwards, K.J., 2008. Iron isotope fractionation in subterranean estuaries. Geochimica Et Cosmochimica Acta, 72: 3413-3430.

Schroth, A.W., Crusius, J., Chever, F., Bostick, B.C., Rouxel, O.J., 2011. Glacial influence on the geochemistry of riverine iron fluxes to the Gulf of Alaska and effects of deglaciation. Geophysical Research Letters, 38:

Schroth, A.W., Crusius, J., Sholkovitz, E.R., Bostick, B.C., 2009. Iron solubility driven by speciation in dust sources to the ocean. Nat. Geosci., 2: 337-340.

Schroth, A.W., Crusius, J., Hoyer, I., Campbell, R., 2014. Estuarine removal of glacial iron and implications for iron fluxes to the ocean. Geophysical Research Letters, 41: 3951-3958.

Schuth, S., Hurrass, J., Munker, C., Mansfeldt, T., 2015. Redox-dependent fractionation of iron isotopes in suspensions of a groundwater-influenced soil. Chemical Geology, 392: 74-86.

Severmann, S., Johnson, C.M., Beard, B.L., McManus, J., 2006. The effect of early diagenesis on the Fe isotope compositions of porewaters and authigenic minerals in continental margin sediments. Geochimica Et Cosmochimica Acta, 70: 2006-2022.

Song, L., Liu, C.-Q., Wang, Z.-L., Zhu, X., Teng, Y., Liang, L., Tang, S., Li, J., 2011. Iron isotope fractionation during biogeochemical cycle: Information from suspended particulate matter (SPM) in Aha Lake and its tributaries, Guizhou, China. Chemical Geology, 280: 170-179.

Vasyukova, E.V., Pokrovsky, O.S., Viers, J., Oliva, P., Dupre, B., Martin, F., Candaudap, F., 2010. Trace elements in organic- and iron-rich surficial fluids of the boreal zone: Assessing colloidal forms via dialysis and ultrafiltration. Geochim. Cosmochim. Acta 74(2), 449–468.

Viers, J., Dupre, B., Polve, M., Schott, J., Dandurand, J.-L., Braun, J.-J., 1997. Chemical weathering in the drainage basin of a tropical watershed (Nsimi-Zoetele site, Cameroon): comparison between organic-poor and organic-rich waters. Chemical Geology, 140: 181-206.

Welch, S.A., Beard, B.L., Johnson, C.M., Braterman, P.S., 2003. Kinetic and equilibrium Fe isotope fractionation between aqueous Fe(II) and Fe(III). Geochimica et Cosmochimica Acta, 67: 4231-4250.

Wu, L.L., Beard, B.L., Roden, E.E., Johnson, C.M., 2011. Stable Iron Isotope Fractionation Between Aqueous Fe(II) and Hydrous Ferric Oxide. Environmental Science & Technology, 45: 1847-1852.

Yesavage, T., Fantle, M.S., Vervoort, J., Mathur, R., Jin, L.X., Liermann, L.J., Brantley, S.L., 2012. Fe cycling in the Shale Hills Critical Zone Observatory, Pennsylvania: An analysis of biogeochemical weathering and Fe isotope fractionation. Geochimica Et Cosmochimica Acta, 99: 18-38.

Figure captions:

Figure 1: Map showing the watersheds of the major rivers discharging in the Arctic Ocean and adapted from (Holmes et al., 2012). Red dots show sampling locations of the Ob' and Lena, Copper River and its tributaries, as well as rivers draining into the White Sea. The Ob', Lena and Severnaya Dvina contribute respectively to 18%, 25% and 4.6% of the total riverine water flux in the Arctic Ocean.

Figure 2: δ^{56}Fe and Fe/Al (g/g) ratios as a function of pore size in filtrates of the White Sea river system for zone 1 (Ruiga #9 and Ladreka #23 and Yukovo area Y-1 to Y-5) and zone 2 (Severnaya Dvina A-3, A-18, A-19 and Pinega A-7). Location and additional data on the samples is given in Table S1 and S4.

Figure 3: δ^{56}Fe and Fe concentrations for dissolved (< 0.45 and 0.22 μm) and soluble (< 0.02 μm) fractions from different tributaries of the Copper River watershed, including glacial, proglacial lake fed, boreal blackwater, and boreal montane. Location and additional data on the samples is given in Table S1 and S5.

Figure 4: Daily discharge measured at Salekhard and Kyusyur stations for Ob' and Lena respectively, δ^{56}Fe values of the Ob' and Lena filtered water collected as part of the Student Partners Project.

Figure 5: δ^{56}Fe values and DOC concentrations of soluble and colloidal fractions from studied Arctic and sub-Arctic watersheds.

Figure

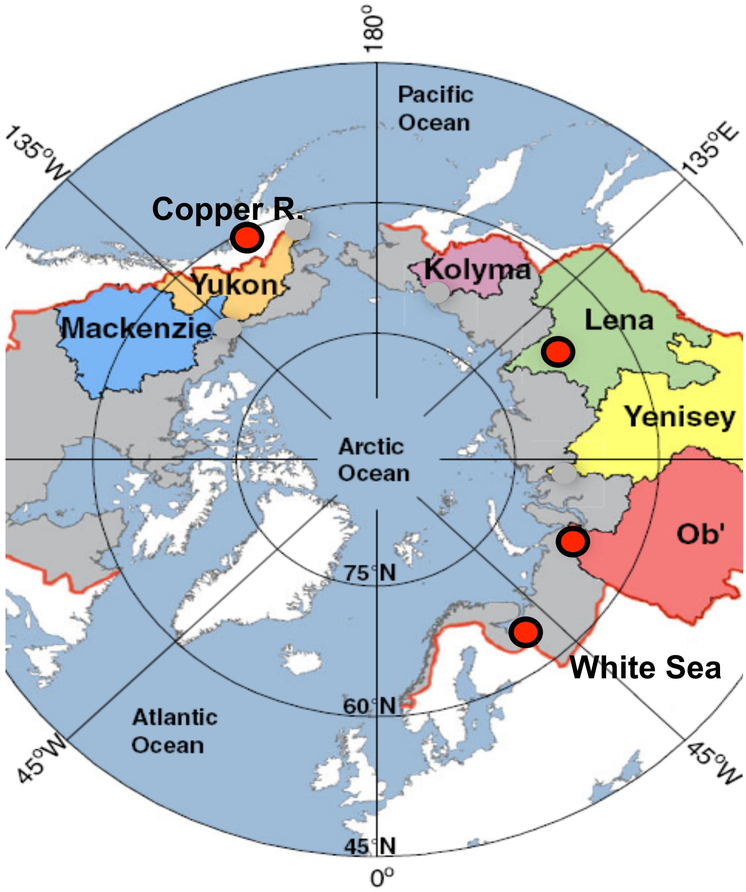

Figure 1

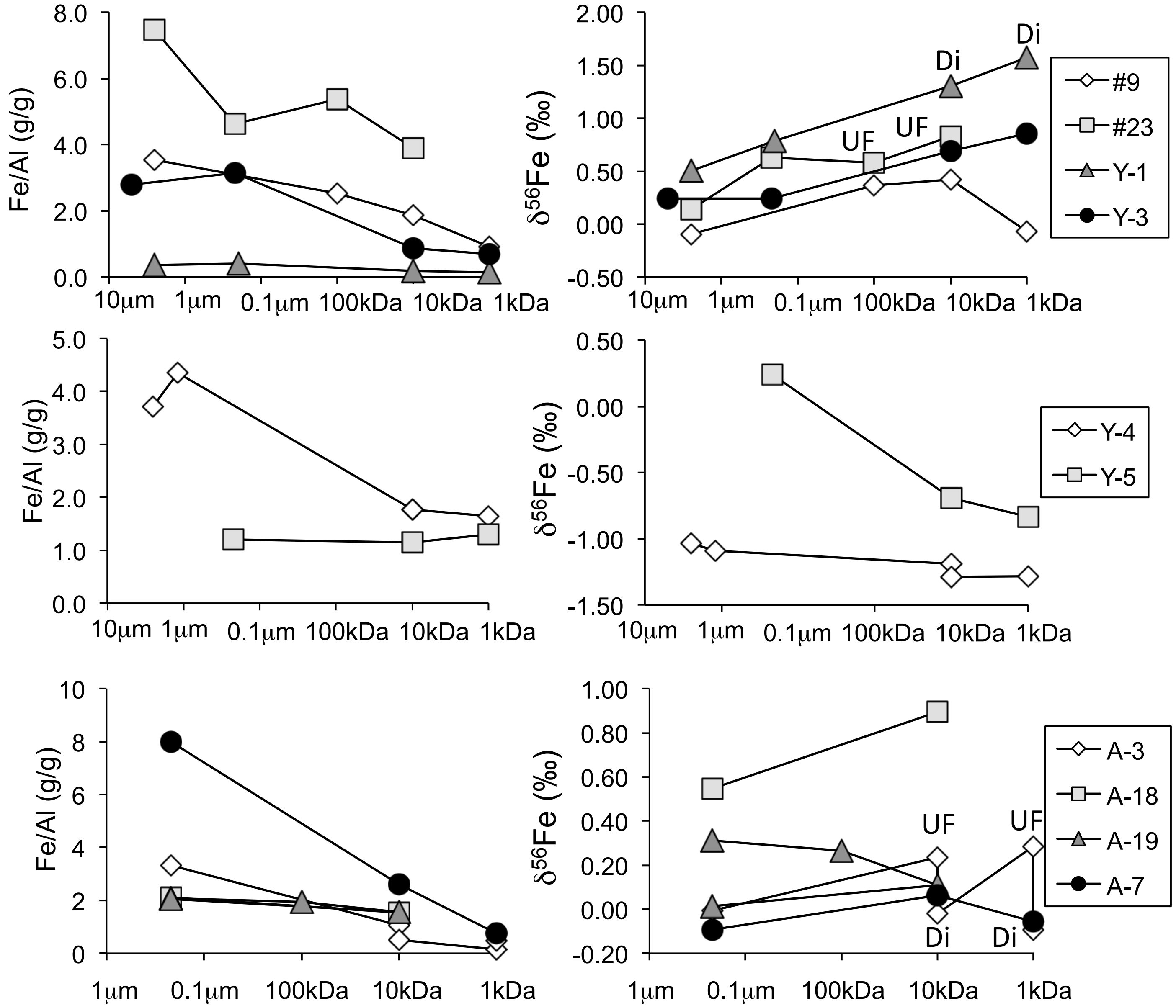

8.0
6.0
4.0
2.0
0.0
Fe/Al (g/g)
10µm 1µm 0.1µm 100kDa 10kDa 1kDa
2.00
1.50
1.00
0.50
0.00
-0.50
δ56Fe (‰)
Di
Di
UF
UF
#9
#23
Y-1
Y-3
5.0
4.0
3.0
2.0
1.0
0.0
0.50
0.00
-0.50
-1.00
-1.50
Y-4
Y-5
10
8
6
4
2
0
1µm 0.1µm 100kDa 10kDa 1kDa
1.00
0.80
0.60
0.40
0.20
0.00
-0.20
UF
UF
Di
Di
A-3
A-18
A-19
A-7

Figure 2

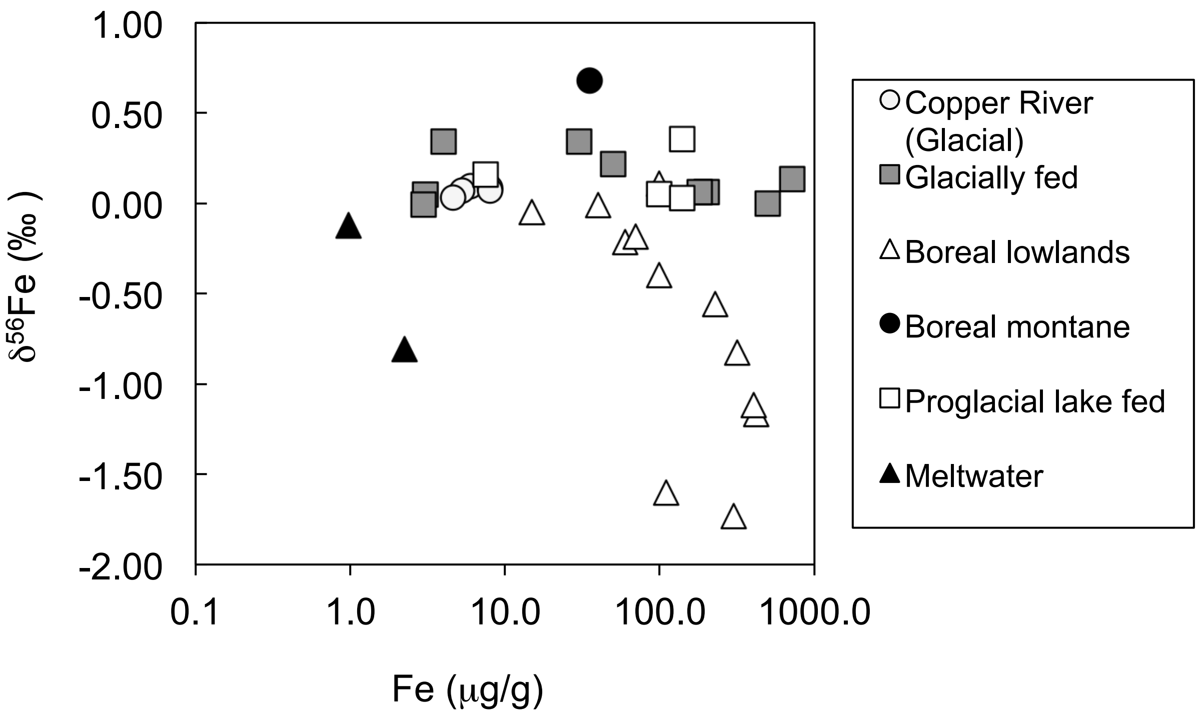

1.00
0.50
0.00
-0.50
-1.00
-1.50
-2.00
δ56Fe (‰)
0.1
1.0
10.0
100.0
1000.0
Fe (μg/g)
Copper River (Glacial)
Glacially fed
Boreal lowlands
Boreal montane
Proglacial lake fed
Meltwater

Figure 3

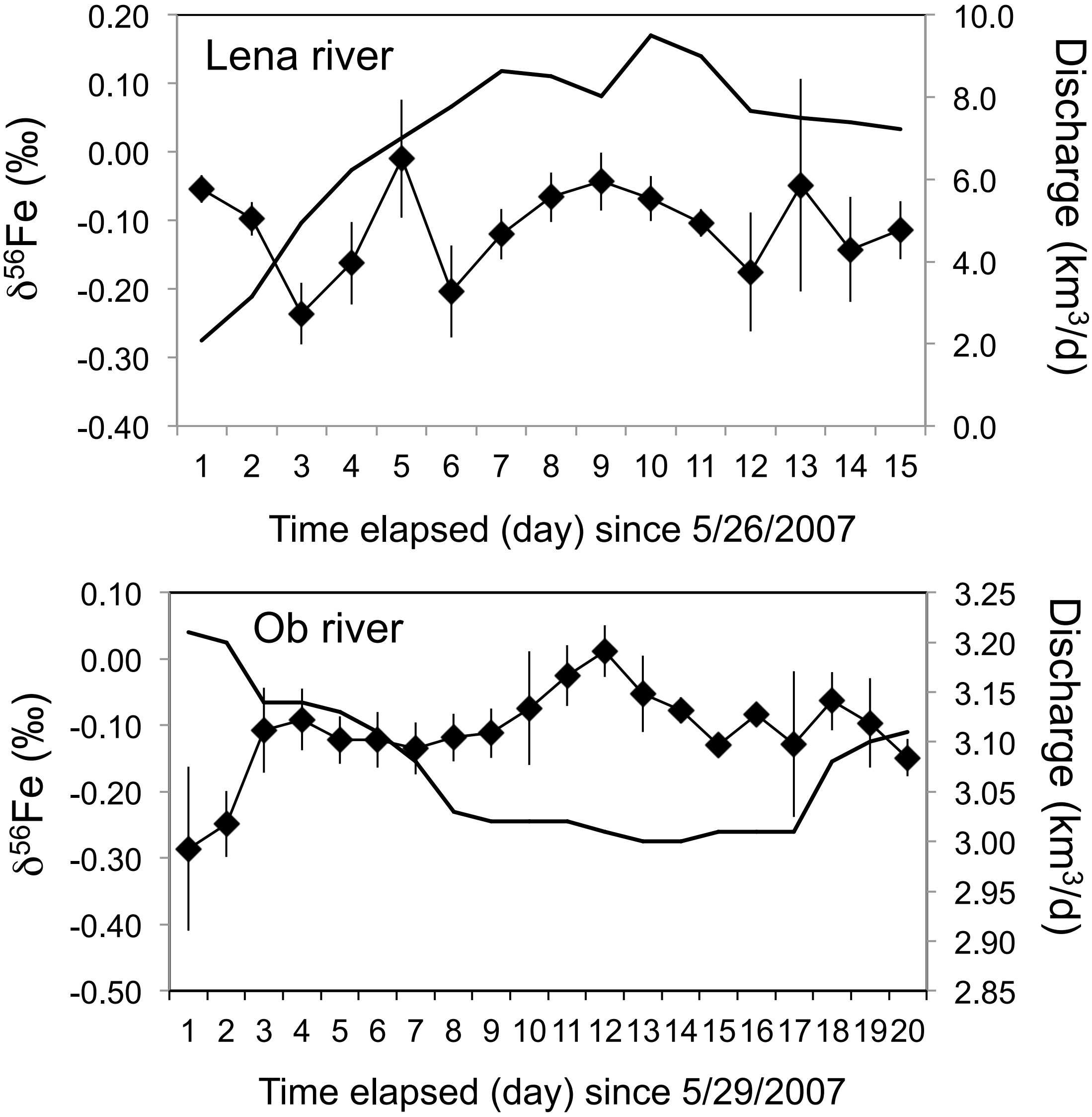
Lena river
0.20
0.10
0.00
-0.10
-0.20
-0.30
-0.40
δ56Fe (‰)
10.0
8.0
6.0
4.0
2.0
0.0
Discharge (km3/d)
1 2 3 4 5 6 7 8 9 10 11 12 13 14 15
Time elapsed (day) since 5/26/2007
Ob river
0.10
0.00
-0.10
-0.20
-0.30
-0.40
-0.50
δ56Fe (‰)
3.25
3.20
3.15
3.10
3.05
3.00
2.95
2.90
2.85
Discharge (km3/d)
1 2 3 4 5 6 7 8 9 10 11 12 13 14 15 16 17 18 19 20
Time elapsed (day) since 5/29/2007

Figure 4

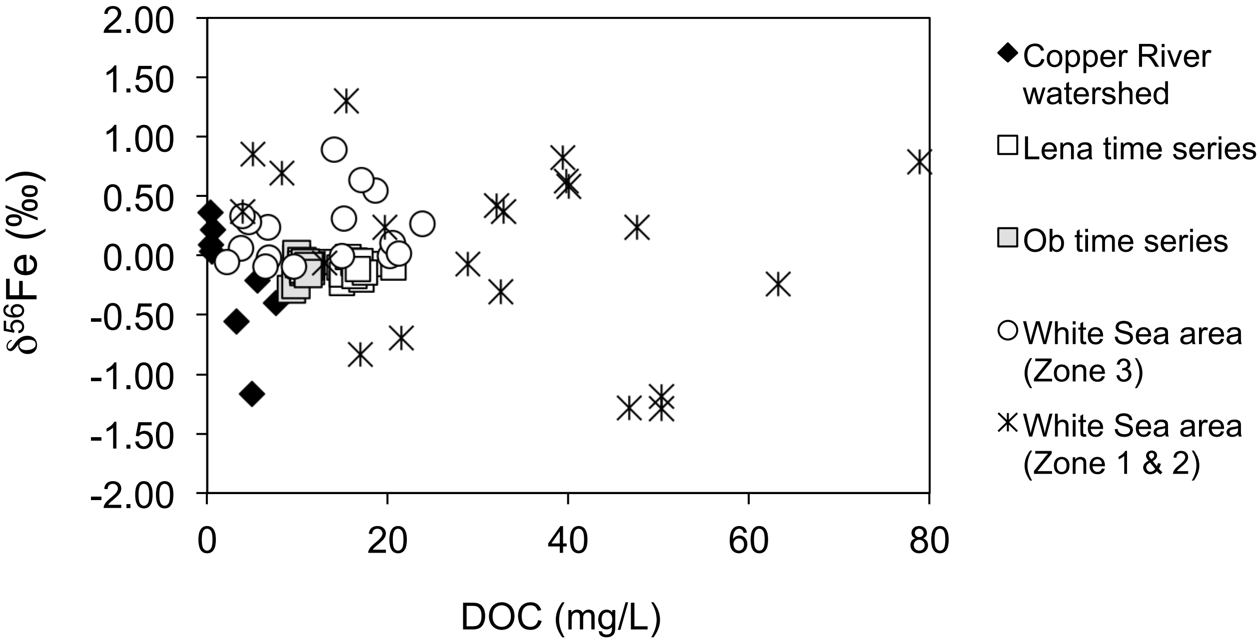
δ56Fe (‰)
2.00
1.50
1.00
0.50
0.00
-0.50
-1.00
-1.50
-2.00
0
20
40
60
80
DOC (mg/L)
Copper River watershed
Lena time series
Ob time series
White Sea area (Zone 3)
White Sea area (Zone 1 & 2)

Figure 5

Supplementary Tables

Table S1: List of sampled waters from the White Sea watershed and their main characteristics

River	Water ID	Lat	Long	Sampling date (d/m/yr)	Type	Flow	Comments	Bedrock Lithology / Tributary type
Zone 1								
Ruiga	9	63°45'43"N	35°47'13"E	25.07.2004	II	BF	Upper reaches	Archean Granite, Marine deposits (sand, clay) and peat
Ladreka	23	64°17'02"N	35°18'52"E	06.08.2004	II	BF	100 m above the bridge, freshwater	
Yukovo	Y-1	64°22'58"N	35°36'36"E	15.02.2006	III	BF	Stagnant surface water under 20 cm of ice	
Yukovo	Y-3	64°21'31"N	35°40'51"E	16.02.2006	III	BF	Stream from wetland zone, under ice 5-7 cm	
Yukovo	Y-2	64°21'19"N	35°40'44"E	15.02.2006	IV	BF	Groundwater (pit)	
Yukovo	Y-4	64°21'39"N	35°40'50"E	16.02.2006	IV	BF	Water lenses trapped in the ice at the tidal zone (connected to Y3)	
Yukovo	Y-5	64°21'37"N	35°40'56"E	16.02.2006	IV	BF	Superficial flow frozen in form of stalactites	
Zone 2								
Peschanaya	S-32	66°12'03"N	43°40'12"E	23.08.2006	III	BF	Small stream (200-300 m length) from coastal wetland zone	Glacial morens (sand) and peat)
Peschanaya	S-40	66°12'00"N	43°32'12"E	24.08.2006	IV	BF	Soil pit water in the coastal bog discharging to the sea	
Zone 3								
Severnaya Dvina	A-3 F	64°40'24"N	40°33'11"E	28.02.2007	I	BF	Ekonomiya monitoring point (13h20)	Carbonate P, K; clays (Q), sand (Q), claystone and sandstone (J, T)
Severnaya Dvina	A-18	64°27'04"N	40°40'54"E	6.05.2007	I	HF	Surface, above the city (M-12 Volodia)	
Severnaya Dvina	A-28	64°00'00"N	41°09'17"E	18.06.2007	I	BF	Above the bridge (Arkhangelsk), left bank	
Ilasskoe Bog	A-19	64°19'40"N	40°36'41"E	7.05.2007	IV	HF	Ombotrophic bog	Ombrotrophic bog (peat deposits) on limestones (K)
Ilasskoe Creek	A-20	64°19'57"N	40°37'35"E	7.05.2007	III	HF	Creek from Ilasskoe bog near the railway	
Pinega	A-7	64°54'56"N	43°27'08"E	2.03.2007	I	BF	Mainstream	Carbonate P, K, gypsum; less amount of clays (Q), sand (Q),
Pinega	A-27	64°54'56"N	43°27'08"E	23.05.2007	I	HF	Mainstream (Golubino)	
Sotka	A-8	64°07'34"N	43°03'54"E	3.03.2007	I	BF	Mainstream	Carbonate P), gypsum (P1), clays (Q), sand (Q)
Sotka	A-25	64°07'34"N	43°03'54"E	22.05.2007	I	HF	Mainstream	

Type I: Large rivers 100 - 500,000 km², Type II: Small rivers , S < 50 km²; Type III: Semi-permanent streams (1 - 10 km²)
Type IV: Stagnant (soil, wetland) water, soil pits close to coast high DOC
BF: Base flow, HF: High Flow

Table S2: List of sampled waters from the Copper River watershed in Alaska and their main characteristics and chemical compositions

River	Water ID	Lat	Long	Type	Sample ID	Filtration	pH	Fe (ug/L)	DOC (mg/L)	δ^{56}Fe	2SD	δ^{57}Fe	2SD	Note
Copper River (CR)														
CR above Chitina river	8	61.529	144.408	GL	AK-07	<0.2um	7.9	600.0		**0.09**	0.09	**0.14**	0.40	
CR below Chitina river	10	61.482	144.452	GL	A22	<0.45um	7.8	530.0		**0.07**	0.06	**0.10**	0.13	*
CR delta channel	26	60.445	145.08	GL	A25	<0.45um	7.9	800.0	0.45	**0.09**	0.06	**0.15**	0.13	*
					AK-09	<0.2um	7.9	798.9		**0.07**	0.06	**0.14**	0.31	
CR above childs glacier	33	60.673	144.755	GL	A14	<0.45um	8.1	460.0		**0.03**	0.06	**0.20**	0.13	*
Copper River tributaries and local waters														
College Creek	13	63.227	145.485	GL	A20	<0.45um	7.9			**0.01**	0.06	**0.00**	0.13	*
Ibeck Creek	27	60.508	145.541	GL	A23	<0.45um	7.5	720.0		**0.13**	0.06	**0.24**	0.13	*
Kotsina River	9	61.581	144.408	GL	A21	<0.45um	7.7	500.0		**0.00**	0.06	**0.02**	0.13	*
Kuskulana River	12	61.556	144.022	GL	A17	<0.45um	8	200.0		**0.06**	0.06	**0.06**	0.13	*
McCarthy Creek	23	61.431	142.926	GL	A16	<0.45um	8	30.0		**0.34**	0.06	**0.26**	0.13	*
Meterasbe River	35			GL	AK-08	<0.2um		3.0		**0.05**	0.17	**0.10**	0.86	
Knik River	34			GL	AK-11	<0.2um		3.0		**-0.01**	0.22	**-0.13**	0.30	
					A18	<0.45um		50.0	0.66	**0.22**	0.06	**0.31**	0.13	*
Strerler Creek	18			GL	AK-04	<0.2um		4.0		**0.34**	0.15	**0.44**	0.26	
Matanuska River	Mat			GL	A15	<0.45um		180.0		**0.06**	0.15	**0.12**	0.32	
Airport Creek	29	60.461	145.293	BB	A11	<0.45um	7.3	230.0	3.2	**-0.56**	0.06	**-0.87**	0.13	*
					AK-03	<0.2um	7.3	317.4		**-0.83**	0.05	**-1.21**	0.14	
					A10	<0.02um	7.3	110.0		**-1.60**	0.06	**-2.37**	0.13	
Eyak River	28	60.529	145.64	BB	A9	<0.45um	7.3	420.0	4.99	**-1.17**	0.06	**-1.71**	0.13	*
					A19	<0.02um	7.3	300.0		**-1.73**	0.15	**-2.58**	0.32	
					AK-13	<0.2um	7.3	402.5		**-1.12**	0.08	**-1.70**	0.20	
Gulkana River	16	62.27	145.385	BB	A5	<0.45um	7.7	60.0	5.56	**-0.21**	0.12	**-0.29**	0.24	*
					A2	<0.02um	7.7	15.0		**-0.05**	0.15	**-0.13**	0.32	
Swampy Creek	31	60.435	145.214	BB	A24	<0.45um	7.4			**-0.03**	0.06	**-0.09**	0.13	*
Tolsona Creek	17	62.101	145.969	BB	A7	<0.45um	7.6	100.0		**0.11**	0.15	**0.07**	0.32	*
					A6	<0.02um	7.6	40.0		**-0.01**	0.12	**0.05**	0.24	
Willow Creek	4	61.817	145.216	BB	A3	<0.45um	7.3	100.0	7.6	**-0.40**	0.15	**-0.69**	0.32	*
					A8	<0.02um	7.3	70.0		**-0.18**	0.06	**-0.32**	0.13	
Tractor Creek	25	61.388	143.197	BM	A4	<0.45um	6.9	35.0		**0.68**	0.12	**0.99**	0.24	
Klutina River	3	61.954	145.322	LK	AK-06	<0.2um	7.4	7.5		**0.16**	0.06	**0.23**	0.16	
Tazlina River	2	62.054	145.426	LK	A12	<0.45um	7.4	140.0	0.35	**0.36**	0.06	**0.51**	0.13	*
					AK-12	<0.2um		99.1		**0.05**	0.10	**0.11**	0.28	
Tonsina River	6	61.663	145.183	LK	A13	<0.45um	7.4	140.0	0.52	**0.03**	0.06	**0.02**	0.13	*
Clear Creek	24			MW	AK-05	<0.2um		1.0		**-0.12**	0.19	**-0.11**	0.56	
Glacial meltwater	St32			MW	AK-02	<0.2um		2.2		**-0.81**	0.23	**-1.21**	0.43	

Sampling date between 8/19/2008 and 8/27/2008

Type "GL": glacial; Type "LK": proglacial lake fed; Type "BB": boreal blackwater; Type "BM": boreal montane, Type "MW": meltwater

(*) Reference from Schroth et al., 2011

Table S3: List of sampled waters from the Lena and Ob and their main characteristics and chemical compositions

River	Water ID	Date (m/d/yr)	Discharge (km3/d)	Water Temp (°C)	DOC (mg/L)	Ca (mg/L)	Sr (ug/L)	Ba (ug/L)	Al (ug/L)	Mn (ug/L)	Fe (ug/L)	**δ^{56}Fe**	2SD	**δ^{57}Fe**	2SD
	SK1	5/26/2007	2.08	5.9	13.11	12.00	128.3	15.96	22.1	66.2	334	**-0.05**	0.02	**0.02**	0.07
	SK2	5/27/2007	3.15	5.2	14.66	12.82	141.1	17.40	24.4	75.0	359	**-0.10**	0.02	**-0.01**	0.16
	SK3	5/28/2007	4.94	5.4	14.97	12.48	129.2	17.07	23.2	76.6	363	**-0.24**	0.05	**-0.32**	0.13
	SK4	5/29/2007	6.22	6.4	14.91	9.69	92.8	14.57	26.1	69.1	443	**-0.16**	0.06	**-0.25**	0.08
	SK5	5/30/2007	7.01	7.4	15.59	9.15	86.8	14.23	27.7	66.6	459	**-0.01**	0.09	**0.14**	0.13
	SK6	5/31/2007	7.78	8.9	17.05	9.53	89.9	14.51	29.2	62.6	457	**-0.20**	0.07	**-0.16**	0.10
	SK7	6/1/2007	8.64	9.7	16.73	9.12	83.2	14.19	29.3	43.8	377	**-0.12**	0.04	**-0.09**	0.11
Lena	SK8	6/2/2007	8.50	13.1	16.20	8.29	83.6	12.57	29.2	33.5	345	**-0.07**	0.04	**0.15**	0.08
	SK9	6/4/2007	8.03	13.7	16.25	9.19	91.9	13.82	29.9	30.9	324	**-0.04**	0.04	**-0.04**	0.08
	SK10	6/5/2007	9.50	9.7	18.22	7.67	70.9	12.61	30.1	24.6	301	**-0.07**	0.03	**-0.04**	0.10
	SK11	6/6/2007	8.99	11.1	20.66	8.96	89.4	13.50	28.6	23.7	287	**-0.10**	0.02	**-0.20**	0.02
	SK12	6/8/2007	7.67	11.1	16.31	9.15	80.0	11.79	29.4	15.5	249	**-0.18**	0.09	**-0.24**	0.09
	SK13	6/9/2007	7.49	9.2	17.00	9.01	75.4	11.83	25.7	14.9	228	**-0.05**	0.16	**-0.04**	0.06
	SK14	6/10/2007	7.38		17.46	7.86	71.1	11.01	25.4	13.7	217	**-0.14**	0.08	**0.03**	0.19
	SK15	6/11/2007	7.23		16.64	9.36	76.5	11.82	21.9	14.6	225	**-0.11**	0.04	**-0.07**	0.02
	SK1	5/29/2007	3.21	6.0	9.37	3.95	27.4	5.12	27.2	90.7	592	***-0.29***	*0.12*	***-0.32***	*0.13*
	SK2	5/30/2007	3.20	6.0	9.86	3.72	24.6	4.60	31.4	118.3	663	***-0.25***	*0.05*	***-0.28***	*0.07*
	SK3	5/31/2007	3.14	7.0	10.79	2.67	18.8	3.78	41.2	95.6	764	**-0.11**	0.06	**-0.18**	0.08
	SK4	6/1/2007	3.14	7.0	11.19	2.80	17.8	3.78	49.2	74.3	746	**-0.09**	0.05	**-0.10**	0.07
	SK5	6/2/2007	3.13	7.0	10.89	2.46	15.5	4.72	36.4	33.3	653	**-0.12**	0.04	**-0.20**	0.04
	SK6	6/3/2007	3.11	5.0	11.16	2.00	13.3	3.54	53.7	41.2	736	**-0.12**	0.04	**-0.13**	0.10
	SK7	6/4/2007	3.08	5.0	10.65	2.15	14.3	5.22	54.1	45.0	843	**-0.13**	0.04	**-0.11**	0.10
	SK8	6/5/2007	3.03	8.0	10.65	1.91	11.8	4.88	50.2	35.2	692	**-0.12**	0.04	**-0.13**	0.10
	SK9	6/6/2007	3.02	9.0	10.70	2.03	12.4	3.48	51.6	27.4	690	**-0.11**	0.04	**-0.28**	0.04
	SK10	6/7/2007	3.02	10.0	10.16	2.42	15.3	3.68	50.8	33.9	657	**-0.07**	0.09	**-0.11**	0.14
Ob'	SK11	6/8/2007	3.02	11.0	9.88	2.05	13.5	4.46	54.7	38.9	637	**-0.03**	0.05	**-0.01**	0.15
	SK12	6/9/2007	3.01	9.0	9.94	2.28	15.8	5.13	55.1	36.3	678	**0.01**	0.04	**-0.10**	0.09
	SK13	6/10/2007	3.00	9.8	10.51	3.68	29.0	7.02	33.4	33.5	533	**-0.05**	0.06	**0.10**	0.05
	SK14	6/11/2007	3.00	10.0	10.48	3.02	21.6	6.15	29.4	18.7	573	**-0.08**	0.02	**-0.13**	0.05
	SK15	6/12/2007	3.01	10.0	11.20	2.07	11.6	3.08	45.2	13.3	667	**-0.13**	0.02	**-0.03**	0.04
	SK16	6/13/2007	3.01	10.0	11.47	2.39	15.5	4.46	39.8	11.1	598	**-0.08**	0.01	**-0.07**	0.01
	SK17	6/14/2007	3.01	11.0	11.48	2.20	14.4	3.59	48.3	15.1	717	**-0.13**	0.11	**-0.13**	0.08
	SK18	6/15/2007	3.08	11.0	10.90	1.99	12.9	3.26	43.1	12.9	486	**-0.06**	0.04	**-0.05**	0.14
	SK19	6/16/2007	3.10	11.5	11.27	3.33	23.5	4.86	39.1	18.3	566	**-0.10**	0.07	**-0.21**	0.08
	SK20	6/17/2007	3.11	11.5	11.21	2.72	18.0	3.96	43.4	19.2	597	**-0.15**	0.03	**-0.12**	0.01

Table S4: Chemical composition and pH of sampled waters from the White Sea watershed for different filtration size

Zone	River	Type / Flow	Water ID	Filtration	pH	DOC (mg/L)	Ca (mg/L)	Mg (mg/L)	Na (mg/L)	Sr (ug/L)	Al (ug/L)	Mn (ug/L)	Fe (ug/L)	δ^{56}Fe	2SD
Zone 1	Ruiga	II / BF	9	<2.5um	5.92	34.4	1.84	2.93	2.23	13.3	749.8	131.5	2660.0	**-0.09**	0.09
				<100kD/UF	6.67	32.8	1.84	2.91	2.29	12.8	717.0	149.4	1805.0	**0.37**	0.09
				<10kD/UF	6.46	32.0	1.82	2.87	2.40	12.5	696.4	145.5	1290.0	**0.42**	0.12
				<1kD/UF	6.75	13.0	1.27	2.36	2.48	8.3	240.8	106.5	219.0	**-0.07**	0.28
	Ladreka	II / BF	23	<2.5um	7.5	41.3	4.23	3.45	33.73	35.0	439.3	115.8	3279.0	**0.14**	0.06
				<0.22um	7.5	39.8	3.93	3.29	34.99	32.1	235.6	118.2	1088.0	**0.63**	0.08
				<100 kD UF	7.47	40.1	4.17	3.40	33.22	33.3	270.4	102.1	1453.0	**0.58**	0.08
				<10kD UF	7.51	39.4	2.30	2.35	31.77	25.6	136.3	72.6	530.6	**0.83**	0.06
	Yukovo & local water	III / BF	Y-1	<2.5 um	6.14	91.2	2.68	6.20	46.86	47.0	1491.0	20.5	535.3	**0.50**	0.03
				<0.2 um		78.9	2.27	4.45	40.15	38.4	1020.6	16.6	404.9	**0.79**	0.03
				<10kD dial		15.4	1.35	3.67	39.02	26.4	370.0	10.2	63.1	**1.31**	0.10
				<1kD dial			1.17	3.22	37.39	21.6	191.8	7.9	24.8	**1.58**	0.13
		IV / BF	Y-2	<0.22 um	7.44	4.0	22.97	8.40	13.22	112.1	1.7	439.6	603.5	**0.37**	0.10
		III / BF	Y-3	<5um	6.04	31.3	3.70	3.12	11.89	34.9	480.2	129.3	1337.2	**0.24**	0.04
				<0.22um		19.7	4.53			34.1	356.9	125.0	1117.3	**0.24**	0.12
				<10kD dial		8.2	2.83	2.66	26.30	29.3	107.2	96.4	93.3	**0.69**	0.09
				<1kD dial		5.1	3.73			28.2	68.1	93.4	46.3	**0.86**	0.14
		IV / BF	Y-4	<2.5 um		76.4	214.46			2983.6	2423.0	1474.5	9016.7	**-1.04**	0.16
				<1.2 um		67.7	49.40			755.5	634.5	409.1	2757.3	**-1.09**	0.05
				<10kD dial		50.3	60.19			740.3	235.1	317.5	416.0	**-1.19**	0.08
				<10kD dial		50.3	60.19			740.3	235.1	317.5	416.0	**-1.29**	0.10
				<1kD dial		46.7	59.00			720.5	170.6	306.1	279.9	**-1.28**	0.06
		IV / BF	Y-5	<0.22 um	3.92	47.6	2.15	0.97	6.68	12.5	890.4	45.3	1072.1	**0.24**	0.03
				<10kD		21.5	1.30			8.9	417.8	32.7	479.6	**-0.69**	0.08
				<1kD dial		17.0	1.07	0.63	5.24	7.7	302.1	28.1	392.8	**-0.83**	0.15
Zone 2	Peschanaya & local water	III / BF	s32	<0.45um	4.18	32.5	0.93	0.88	4.07	7.3	192.2	39.1	816.7	**-0.30**	0.08
		IV / BF	s40	<0.45 um	4.43	63.2	0.85	1.15	5.49	8.9	99.6	4.4	350.2	**-0.24**	0.13
				<1 kD UF		28.8	0.96	0.91		6.7	49.2	4.0	107.7	**-0.07**	0.08
Zone 3	Severnaya Dvina	I / BF	A-3	<0.22um	7.17	14.9	37.36	8.62	14.03	375.5	112.3	44.2	372.8	**-0.01**	0.09
				<10kD UF		6.7	37.25	8.44	14.26	390.3	58.8	44.3	62.8	**0.24**	0.07
				<10kD dial		6.8	36.58	8.28	14.05	380.6	36.5	40.3	18.9	**-0.02**	0.03
				<1kD UF		4.6	33.43	7.53	12.72	355.6	34.5	37.9	5.0	**0.28**	0.12
				<1kD dial		9.6	35.86	8.13	13.76	375.1	34.8	40.1	16.3	**-0.09**	0.10
		I / HF	A-18	<0.22 um	7.66	18.6	11.60	2.81	1.75	106.6	268.8	36.6	564.7	**0.55**	0.09
				<10kDa UF		14.1	11.11	2.63	1.69	103.0	57.9	12.5	89.0	**0.89**	0.10
		I / BF	A-28	<0.22 um		20.2	18.52	4.09	4.50	163.0	40.7	24.6	231.9	**-0.01**	0.08
		IV / HF	A-19	<0.22 um	4.15		0.31	0.22	1.34	2.2	112.1	8.4	232.3	**0.31**	0.06
				<100kDa UF		23.8	0.30	0.21	1.29	2.2	98.9	7.0	192.5	**0.27**	0.06
				<10kDa UF		20.5	0.23	0.18	1.25	1.6	55.8	6.1	87.0	**0.11**	0.10
		III / HF	A-20	<0.22 um	4.22	21.2	0.29	0.19	1.09	2.0	110.9	10.2	226.8	**0.01**	0.08
	Pinega	I / BF	A-7	<0.22 um	7.34	6.5	44.75	9.90	9.22	1041.4	17.2	22.4	137.8	**-0.09**	0.11
				<10kD UF		3.8	43.96	9.74	9.18	1051.0	9.7	21.6	25.4	**0.06**	0.04
				<1kD UF		2.2	39.46	8.78	8.60	953.7	17.0	18.9	12.8	**-0.05**	0.04
		I / HF	A-27	<0.22 um		17.1	11.11	2.36	1.37	166.4	116.5	4.1	150.2	**0.64**	0.21
	Sotka	I / BF	A-8	<0.22 um	7.61	3.9	319.48	14.81	4.66	3797.5	6.3	16.8	36.3	**0.34**	0.06
		I / HF	A-25	<0.22 um	7.55	15.1	122.70	3.99	1.28	1099.0	87.8	22.1	231.2	**0.31**	0.17

Type I: Large rivers 100 - 500,000 km², Type II: Small rivers , S < 50 km²; Type III: Semi-permanent streams (1 - 10 km²)
Type IV: Stagnant (soil, wetland) water, soil pits close to coast high DOC
BF: Base flow, HF: High Flow

Supplementary Materials

Methods

Sample filtration

In this study, we operationally defined "dissolved iron", as the fraction passing through 0.45 or 0.22 μm filter size. In some cases, we also used larger pore size filtration at 5, 3 and 2.5 μm to recover together small particles and dissolved Fe fraction. The colloidal and truly dissolved fractions (i.e. < 1 kDa) are obtained using ultra filtration and dialysis methods. For Lena and Ob' river waters, the samples were collected from a small boat and immediately filtered through 0.45 μm filters. Filtered waters were stored in Nalgene high-density polyethylene (HDPE) and frozen until further analysis as described in (Holmes et al., 2012). Samples from Alaska were collected following the ultra clean method of Shiller (2003) and further described in Schroth et al. (2011) where Fe partitioning in river water is determined as soluble (< 0.02 μm) and colloidal (< 0.45 or 0.2 μm) size fractions using trace metal clean syringe filtration of small volume samples (~15 mL to 30 mL) (Shiller, 2003).

The White Sea samples were collected from the middle of the flow channel, using 1 liter HDPE containers held out from the beach on a non-metallic stick. The samples were collected and manipulated as described elsewhere (Ilina et al., 2013, Pokrovsky et al., 2012, Pokrovsky et al., 2010, Vasyukova et al., 2010). Water samples were immediately filtered on-site through sterile, single-use filter units (Sartorius, acetate cellulose filter) with pore sizes of 5, 2.5, 0.45 and 0.22 μm. The first 50 ml of the filtrate was systematically discarded before sampling. Two techniques of ultra-filtration (100 kDa, 10 kDa and 1 kDa) have been used: (1) frontal ultrafiltration (UF) was carried out using a 50-ml polycarbonate cell (Amicon) equipped with a suspended magnet stirring bar located beneath the filter to prevent clogging during pressure filtration at 3 bars; (2) in-situ dialysis filtration involved the use of trace-metal clean SpectraPor 7® dialysis membranes containing ultrapure MQ deionized water placed in flotation in natural water during more than 24h (Vasyukova et al., 2010).

Analysis

Major and trace element analyses were all performed on samples acidified at pH 2 with ultrapure double-distilled HNO_3. Trace element analyses were measured by HR-ICP-MS either at LMTG (France) or WHOI (USA). The riverine water reference material SLRS-4 (National Research Council of Canada) was used to check the accuracy and reproducibility of each analysis. Samples for dissolved organic carbon (DOC) analysis were collected in pyrolyzed sterile Pyrex glass tubes after filtration trough 0.45 or 0.22 μm and analyzed using a Total Carbon Analyzer (Shimadzu TOC 5000).

The procedure for Fe-isotope analysis follows previously described methods in (Escoube et al., 2009) for riverine and brackish waters. In short, acidified samples are evaporated to dryness at 80°C with distilled HNO_3 and H_2O_2 (ultrapure grade) on a hot plate to release the iron from organic complexes. The samples are then purified through anion exchange resin (AG1-X8, Bio-rad). Iron isotope compositions were determined with a *Neptune* (Thermo-Scientific) multicollector inductively coupled plasma mass spectrometry (MC-ICPMS) operating at WHOI and IFREMER using medium or high-resolution mode. Instrumental mass bias is corrected using $^{62}Ni/^{60}Ni$ isotope ratio as internal standard simultaneously measured. All analyses are reported in delta notation relative to the IRMM-014 standard, expressed as $\delta^{56}Fe$, which represents the deviation in per mil relative to the reference material. As $\delta^{56}Fe$ and $\delta^{57}Fe$ are on a single mass fractionation line (r^2= 0.9956), only $\delta^{56}Fe$ values are reported in this paper.

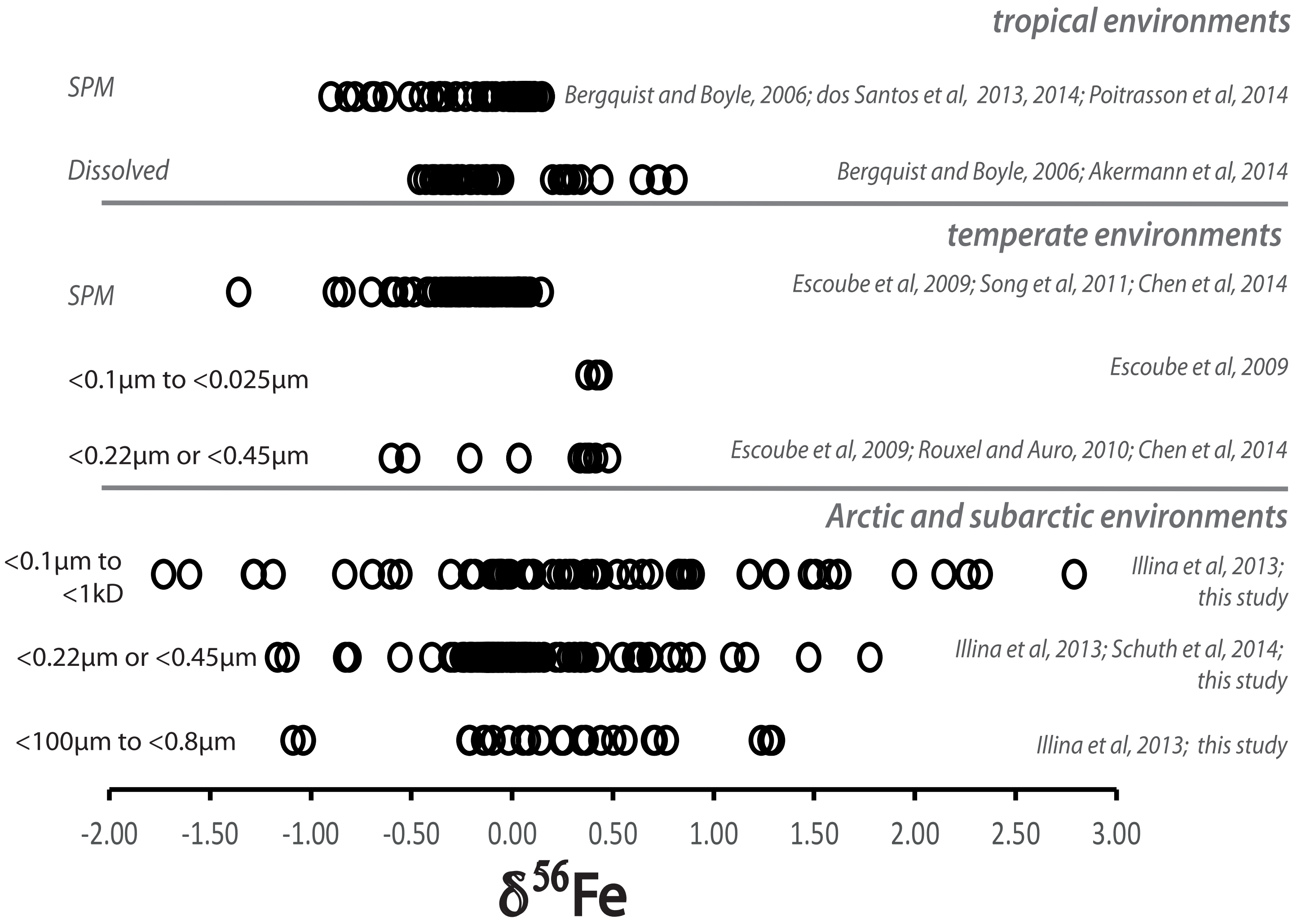

Figure S1: Compilation of Fe isotope composition of rivers reported in the literature: (i) Arctic and subarctic environments including russian rivers, ponds and swamps of the White Sea basin, and Ob' and Lena rivers (Illina et al, 2013; this study), and alaskan rivers (Schroth et al, 2011, this study). ; (ii) Temperate environments include the North River (USA; Escoube et al, 2009); Seine river (France; Chen et al, 2014); Aha lake and its inflowing rivers (China; Song et al, 2011); (iii) Tropical environments including the Amazon River and tributaries (Bergquist and Boyle, 2006; Poitrasson et al, 2014 ; dos Santos Pinheiro et al, 2013, 2014) and Mendong (Cameroon; Akermann et al, 2014). Note that results from Ingri et al (2006) have not been included since they correspond to saturated filters collecting both particles and some class of colloids. SPM corresponds to suspended particulate matter retained on filters of 0.22µm or 0.45µm pore size.

Cited references

Akerman, A., Poitrasson, F., Oliva, P., Audry, S., Prunier, J., Braun, J.J., 2014. The isotopic fingerprint of Fe cycling in an equatorial soil-plant-water system: The Nsimi watershed, South Cameroon. Chemical Geology, 385: 104-116.

Bergquist, B.A., Boyle, E.A., 2006. Iron isotopes in the Amazon River system: Weathering and transport signatures. Earth and Planetary Science Letters, 248: 54-68.

Chen, J.B., Busigny, V., Gaillardet, J., Louvat, P., Wang, Y.N., 2014. Iron isotopes in the Seine River (France): Natural versus anthropogenic sources. Geochimica Et Cosmochimica Acta, 128: 128-143.

Escoube, R., Rouxel, O.J., Sholkovitz, E., Donard, O.F.X., 2009. Iron isotope systematics in estuaries: The case of North River, Massachusetts (USA). Geochimica Et Cosmochimica Acta, 73: 4045-4059.

Holmes, R.M., McClelland, J.W., Peterson, B.J., Tank, S.E., Bulygina, E., Eglinton, T.I., Gordeev, V.V., Gurtovaya, T.Y., Raymond, P.A., Repeta, D.J., Staples, R., Striegl, R.G., Zhulidov, A.V., Zimov, S.A., 2012. Seasonal and Annual Fluxes of Nutrients and Organic Matter from Large Rivers to the Arctic Ocean and Surrounding Seas. Estuaries and Coasts, 35: 369-382.

Ilina, S.M., Poitrasson, F., Lapitskiy, S.A., Alekhin, Y.V., Viers, J., Pokrovsky, O.S., 2013. Extreme iron isotope fractionation between colloids and particles of boreal and temperate organic-rich waters. Geochimica Et Cosmochimica Acta, 101: 96-111.

Ingri, J., Malinovsky, D., Rodushkin, I., Baxter, D.C., Widerlund, A., Andersson, P., Gustafsson, Ö., Forsling, W., Öhlander, B., 2006. Iron isotope fractionation in river colloidal matter. Earth and Planetary Science Letters, 245: 792-798.

Pinheiro, G.M.D., Poitrasson, F., Sondag, F., Vieira, L.C., Pimentel, M.M., 2013. Iron isotope composition of the suspended matter along depth and lateral profiles in the Amazon River and its tributaries. Journal of South American Earth Sciences, 44: 35-44.

Pinheiro, G.M.D., Poitrasson, F., Sondag, F., Cochonneau, G., Vieira, L.C., 2014. Contrasting iron isotopic compositions in river suspended particulate matter: the Negro and the Amazon annual river cycles. Earth and Planetary Science Letters, 394: 168-178.

Pokrovsky, O.S., Viers, J., Dupre, B., Chabaux, F., Gaillardet, J., Audry, S., Prokushkin, A.S., Shirokova, L.S., Kirpotin, S.N., Lapitsky, S.A., Shevchenko, V.P., 2012. Biogeochemistry of carbon, major and trace elements in watersheds of northern Eurasia drained to the Arctic Ocean: The change of fluxes, sources and mechanisms under the climate warming prospective. Comptes Rendus Geoscience, 344: 663-677.

Pokrovsky, O.S., Viers, J., Shirokova, L.S., Shevchenko, V.P., Filipov, A.S., Dupre, B., 2010. Dissolved, suspended, and colloidal fluxes of organic carbon, major and trace elements in the Severnaya Dvina River and its tributary. Chemical Geology, 273: 136-149.

Poitrasson, F., Vieira, L.C., Seyler, P., Pinheiro, G.M.D., Mulholland, D.S., Bonnet, M.P., Martinez, J.M., Lima, B.A., Boaventura, G.R., Chmeleff, J., Dantas, E.L., Guyot, J.L., Mancini, L., Pimentel, M.M., Santos, R.V., Sondag, F., Vauchel, P., 2014. Iron isotope composition of the bulk waters and sediments from the Amazon River Basin. Chemical Geology, 377: 1-11.

Schroth, A.W., Crusius, J., Chever, F., Bostick, B.C., Rouxel, O.J., 2011. Glacial influence on the geochemistry of riverine iron fluxes to the Gulf of Alaska and effects of deglaciation. Geophysical Research Letters, 38: doi 10.1029/2011gl048367

Shiller, A.M., 2003. Syringe filtration methods for examining dissolved and colloidal trace element distributions in remote field locations. Environmental Science & Technology, 37: 3953-3957.

Song, L.T., Liu, C.Q., Wang, Z.L., Zhu, X.K., Teng, Y.G., Liang, L.L., Tang, S.H., Li, J., 2011. Iron isotope fractionation during biogeochemical cycle: Information from suspended particulate matter (SPM) in Aha Lake and its tributaries, Guizhou, China. Chemical Geology, 280: 170-179.

Vasyukova, E.V., Pokrovsky, O.S., Viers, J., Oliva, P., Dupre, B., Martin, F., Candaudap, F., 2010. Trace elements in organic- and iron-rich surficial fluids of the boreal zone: Assessing colloidal forms via dialysis and ultrafiltration. Geochimica Et Cosmochimica Acta, 74: 449-468.